ASIAN JOURNAL OF CIVIL ENGINEERING (BHRC) VOL. 18, NO. 4(2017)
PAGES 643-656

A NUMERICAL INVESTIGATION OF LOCAL – DISTORTIONAL – LATERAL - TORSIONAL BUCKLING INTERACTION OF COLD - FORMED STEEL LIPPED CHANNEL BEAMS

M. Anbarasu*
Department of Civil Engineering, Government College of Engineering, Salem - 636 011, Tamilnadu, India

Received: 22 September 2016; **Accepted:** 9 December 2016

ABSTRACT

This work aims at investigating the buckling behaviour of cold-formed steel (CFS) lipped channel (LC) beams undergoing local(L)-distortional(D)-lateral-torsional (LT) buckling mode interaction for the sake of developing an analytical model to calculate the ultimate resistance to bending moment. The section geometries are identified to have nearly equal elastic local, distortional and lateral-torsional buckling moment values by performing elastic buckling analysis. The identified sections satisfy the condition for prequalified sections in AISI-S100-2007. A finite-element model has been developed and verified against the available test data for cold-formed steel lipped channel sections subjected to the major axis bending. Parametric studies were carried out to investigate the influence of geometries and yield stress values. The numerical results are compared with design predictions from the Direct Strength Method (DSM) in North American specifications for cold-formed steel structures. Based on the comparisons, design recommendations are introduced for cold-formed steel lipped channel beams which experiencing local/distortional/lateral-torsional buckling mode interaction.

Keywords: Buckling interaction; distortional buckling; local buckling; lateral - torsional buckling, lipped channel beam; local - distortional – lateral - torsional buckling interaction.

1. INTRODUCTION

The cold-formed thin-walled beams with open cross section can exhibit different modes of instabilities, namely local, distortional, bending, lateral-torsional buckling and interaction between the above buckling modes. Cold-formed steel lipped channel beams undergo local buckling in the relatively short-wavelength and Distortional buckling occurs in intermediate between that of local buckling and lateral-torsional buckling. Lateral-torsional buckling

*E-mail address of the corresponding author: gceanbu@gmail.com (M. Anbarasu)

occurs long half-wavelength when the cross section buckles without distortion. The three generic forms of buckling of beams are local (L), distortional (D) and lateral-torsional (G) buckling, generally have different wavelengths. However, there is an possibility of interaction among these buckling modes at a certain span length. At that length their post-buckling behaviour, ultimate moments and failure mechanisms are influenced by these three buckling modes.

Put et al. [1] conducted tests on lateral buckling of simply supported and unbraced coldformed steel lipped C channel and Z sections to study the effect of interactions between all the three modes on the strength of beams. Pi et al. [2] developed improved design rules for lateraldistortional buckling based on the numerical study on inelastic behaviour and strengths of coldformed steel beams. Yu and Schafer [3-4] conducted tests on C and Z sections to demonstrate the interaction of local and distortional buckling. Yu and Schafer [5], conducted experiments on lipped channel and lipped zee sections and found the influence of a linear bending moment gradient on the distortional buckling of single-span cold-formed steel beams, and used their finding to explicitly demonstrate the loss of capacity that occurs in the distortional buckling limit state. Silvestre and Camotim [6] proposed closed-formed equation for distortional buckling of C and Z shape beams, based on simplified assumptions. Schafer [7] developed Direct Strength Method (DSM) for the design of thin-walled cold-formed steel columns and beams including distortional buckling mode.

Kurniawan and Mahendran [8] proposed design equations for Lateral Buckling Strength of Simply Supported Lite Steel Beams Subject to Moment Gradient Effects. Dinis and Camotim [9] have estimated the local/distortional mode interaction concerning the post-buckling behavior of a cold-formed steel lipped channel beams subjected to uniform major axis bending, using the shell finite element analysis in ABAQUS. And conclude that, in the flange triggered beams, the pure local initial imperfections are the most detrimental ones, in the sense that they lead to the lowest beam post-buckling strengths and ultimate moments. The web triggered beams may exhibit a fair amount of elastic–plastic strength, reserve, and ductility before collapse. Moreover, the most detrimental initial imperfections are now the pure distortional ones with outward flange-lip motions.

Nandini and Kalyanaraman [10] reported DSM design procedure for LC beams undergoing the interaction of local, distortional and overall lateral torsional buckling, based on Euro code specifications. Kankanamge and Mahendran [11] reported a design equation to calculate the lateral-torsional buckling strength of lipped channel beams subjected to uniform bending. Laim et al. [12] studied the flexural Behaviour of Cold-formed steel beams and examined the current codal specifications. Niu et al. [13] provided experimental evidence for cold-formed stainless steel channel-beams, concerning the distortional-global interaction. Kandasamy et al. [14] conducted tests on flexural-Torsional-Buckling of cold-formed lipped channel beams under restrained boundary conditions and examined the codal provisions. Anbarasu [15] investigated the local (L) - distortional (D) buckling interaction in lipped channel beams and proposed DSM based new design equation, accounting the L-D interaction. Szymczak and Kujawa [16] extensively studied the local buckling of lipped channel beams and proposed new design formulations. The review of the literature shows that buckling interaction studies of cold-formed steel beams are limited.

This research aims at investigating the L-D-LT interaction buckling behaviour in lipped

channel beams subjected to uniform bending. A nonlinear finite element (FE) model is developed herein to simulate the experimental results reported by Kankanamge [17]. The effects of the cross-section geometries and the yield stress values on the behaviour and flexural strength of lipped channel beams are investigated by means of a numerical parametric study. The beam cross-section dimensions and lengths were identified, by means of G_{BTUL}-2.0β [18] and CUFSM [19] elastic buckling analysis, to ensure strong local-distortional-lateral-torsional interaction (nearly coincident local, distortional and lateral-torsional buckling moment). Totally 60 analysis was done on 12 beams with pinned-warp free end conditions. Selected sections satisfy the prequalified section conditions in AISI-S100:2007 [20]. The numerical ultimate moments were compared with ultimate moment predicted by Direct Strength Method (DSM). Finally, the new design equation was proposed to evaluate the strength of beams failing under L-D-LT interaction modes.

2. METHODOLOGY

2.1 Finite element modelling

The numerical model implemented in the multi-purpose FE-based software ABAQUS version 6.10 [21] was used as a simulation tool. The finite element (FE) modeling approach followed the similar pattern as those reported by Kankanamge and Mahendran [11] and Anbarasu [15]. The thin shell element with four nodes and five degrees of freedom per node, S4R5 element were used to discretize the model. The mesh size of approximately of 5x5 mm (length by the width) was used in this study [11]&[15].

The material properties used in the verification model are identical to the FEA as described in Kankanamge [17] were presented in Table1. Residual stresses were ignored. An elastic-perfect plastic model based on a simplified bilinear stress-strain curve without strain hardening was assumed in the parametric study finite element model. For all parametric finite element models, young modulus E = 210000 MPa and Poisson's ratio = 0.3 were used. They simply supported lipped channel beams subjected to a quarter point loadings applied upwards in the shear centre of beams were tested by Kankanamge [17] was simulated in the validation finite element model with loading and boundary condition is shown in Fig. 1(a).

The developed FE model for parametric study with idealized boundary condition and loading is shown in Fig. 1(b). Initial local, distortional and global geometric imperfections were included in the parametric model. But, only global (lateral-torsional) imperfection is included in the validation model. The maximum amplitude of local and distortional mode imperfections were 0.34*t, 0.94*t and L/1000 were used in the parametric model as recomendad by Schafer and Pekoz [22] to initiate the nonlinear analyses. The RIKS method in ABAQUS was used in the nonlinear analysis.

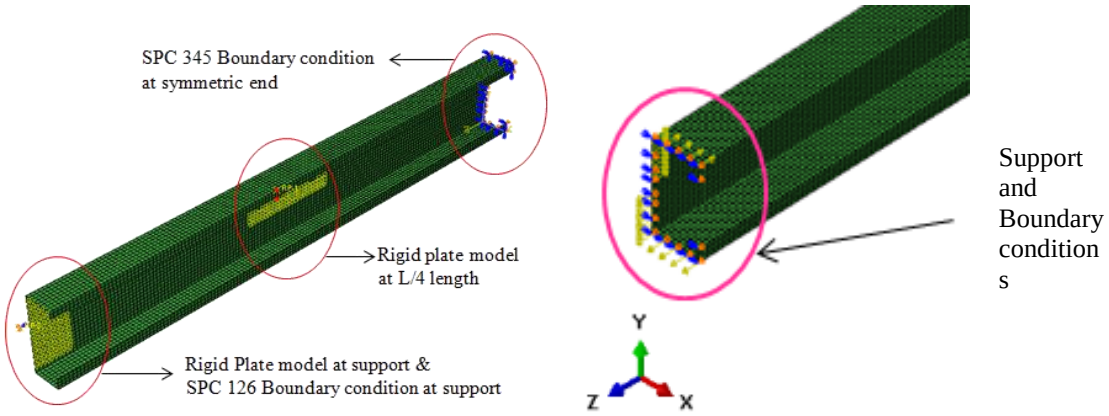

(a) Validation model (b) Parametric model

Fig. 1 Loading and boundary condition

2.2 Validation

The developed model was validated for uniform bending by comparing the numerical results with results obtained experimentally by Kankanamge [17]. Four specimens are subjected to quarter point loading from the experiments are modelled by using the FE analysis. Table 1 shows the comparison of experimental ultimate moment, and those calculated by FE models and show a reasonable agreement between the FE analysis and the experiments. The mean ratio of the ultimate moment capacity of the finite element model and experiment was 0.952 with a standard deviation of 0.017.

Table 1: Comparison of experimental and FEA ultimate moment capacities

Specimen ID (As per literature)	Test Beam Dimensions (mm)					f_y (MPa)	E (GPa)	Ultimate Moment (kNm)		$M_{u,test}/M_{FEA}$
	b	d	l	t	L			$M_{u,test}$	$M_{,FEA}$	
G450-1.9-1500	37.82	107.85	13.48	1.886	1500	515	206	5.13	5.29	0.969
G450-1.9-2000	38.40	108.87	13.46	1.886	2000	515	206	4.44	4.66	0.952
G450-1.9-2500	39.78	107.97	13.77	1.886	2500	515	206	4.01	4.28	0.936
Mean										0.952
Standard Deviation										0.017

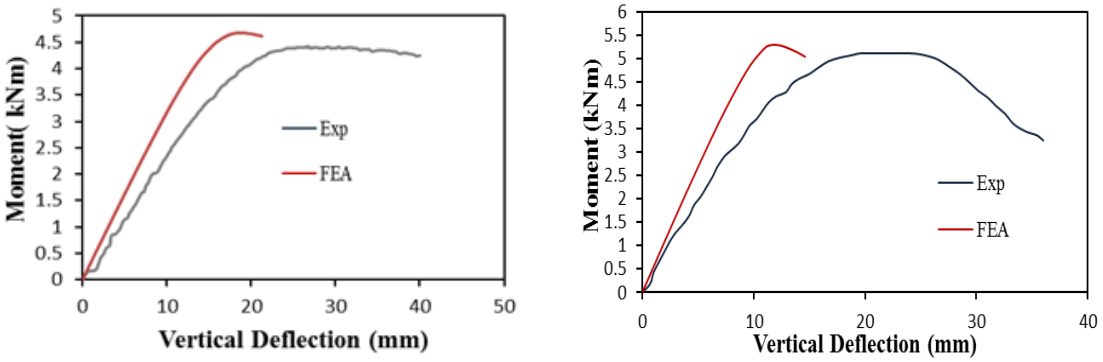

(a) For G450-1.9-2000 (b) For G450-1.9-1500

Fig. 2 Comparison of moment VS vertical deflection

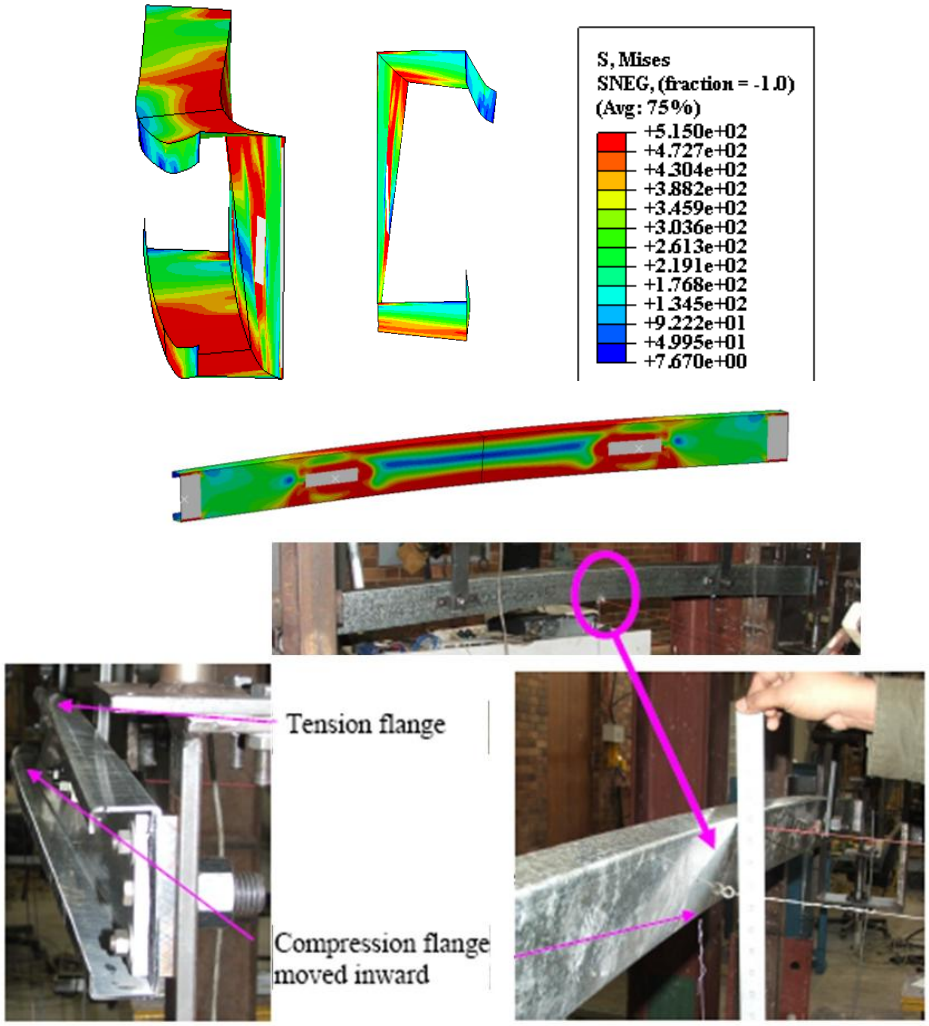

Fig. 3 Comparison of failure modes from the test and FE modelling for G450-1.9-1500

The numerical bending moment versus vertical deflection curves for some of the tested beams is compared with experimental curves in Fig. 2. The comparison agrees fairly well. Fig. 3 shows the comparison of predicted failure mode of 200x45x1.6 tested beam with a finite element model. This compares well with the observed lateral-torsional buckling failure in the experimental study. The agreement can be seen between the experimental and FEA results. Fig. 4 shows the final failure mode of the specimen G450-1.9-2000 from the finite element analysis.

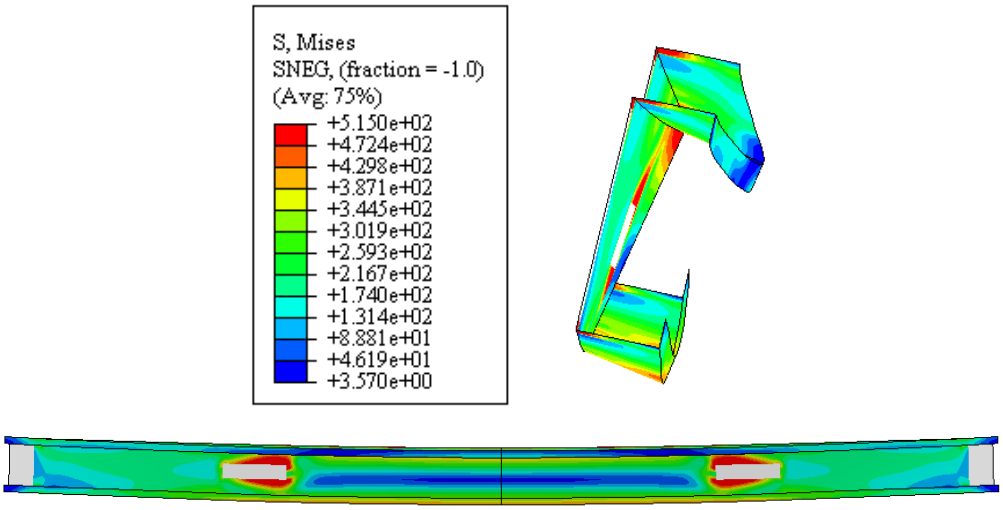

Fig. 4 Failure mode from the FE modelling for G450-1.9-2000

2.3 Section design

The identification of a set of lipped channel beam geometries (cross-section dimensions and length) corresponding to nearly coincidental local, distortional and lateral torsional buckling moments were done by using the code GBTUL [18] and CUFSM [19]. The criterion adopted to ensure the near coincidence of M_{crl}; M_{crd} and M_{cre} is that the ratio between the highest and lowest of these three values does not exceed 1.097 (it is smaller in all cases). The variation of the critical buckling moment M_{cr} with length L (logarithmic scale) for the beam 200x75x15 is presented in Fig. 5. The local buckling mode has a minimum at 100 mm in half-wavelength and the distortional mode has a minimum at 700mm in half-wavelength. It is clearly observed from the Fig. 5 at the length of L = 3600mm, the beam has nearly coincident local, distortional and lateral-torsional buckling moments: M_{crl} = 4.333 kNm, M_{crd} = 4.466 kNm, M_{cre} = 4.430 kNm.

The interaction of L, D and LT buckling modes may significantly reduce the flexural strength, which is estimated on the assumption that the beam fails either in L or D or LT buckling mode without buckling mode interaction. The details of the selected section geometries with buckling moments for E = 210 GPa and ν = 0.3 are summarised in Table 3.

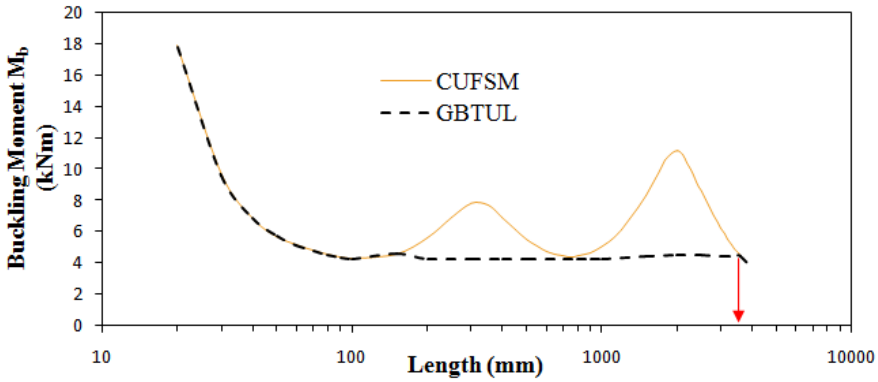

Fig. 5 M_b vs L Curve for LC-4 (200x75x15)

Table 2: Section geometries and buckling moments

Specimen ID	Section Dimensions (mm)					Critical Moments (kNm)			M_{crl} / M_{crd}/ M_{cre} (Max./Min.)
	Web depth (h)	Flange width (b)	Lip depth (l)	thickness (t)	Length (L)	M_{crl}	M_{crd}	M_{cre}	
LC1	100	60	15	1.2	1900	3.877	3.910	3.80	1.029
LC2	120	50	15	1.1	1620	4.345	4.337	4.58	1.056
LC3	120	65	15	1.2	2260	4.324	4.312	4.73	1.097
LC4	200	75	15	1.1	3600	4.333	4.466	4.43	1.031
LC5	115	60	15	1.1	2160	3.492	3.480	3.74	1.075
LC6	125	50	15	1.1	1660	4.417	4.395	4.57	1.040
LC7	180	50	10	1.1	2080	3.847	3.822	3.82	1.007
LC8	150	50	15	1.2	1700	5.848	5.836	5.91	1.013
LC9	150	65	15	1.1	2600	4.164	4.153	4.26	1.026
LC10	185	75	15	1.1	3500	4.239	4.197	4.26	1.015
LC11	100	50	15	1.1	1544	3.698	3.691	3.70	1.002
LC12	130	50	15	1.1	1700	4.442	4.429	4.66	1.052

3. RESULTS - PARAMETRIC STUDY

The primary aim of the parametric studies was to investigate the influence of section geometries and yield stress values on the beam load carrying capacity. The obtained results were also used to assess the DSM beam design equations. The h/b ratio of the selected sections ranges from 1.67 to 3.6. The d/t ratios of selected sections are in the range of 9.09-13.64. The b/t ratios of selected sections are in the range of 41.67-68.18. The h/t ratios of selected sections are in the range of 83.33-181.82. In total 60 finite element analysis were

conducted by varying the five yield stress values, from 250 – 590 MPa on the beam models.

The ratio of Young's modulus to yield stress values of the parametric models considered are in the range of $355 \leq E/f_y \leq 840$. The limit specified in DSM for pre-qualified beams is $E/f_y > 421$. 24 beams analysed in the parametric study do not satisfy the material requirement, but the ultimate moments of these beams also included to examine the DSM provisions to cover wide range of slenderness. The beam ultimate moment obtained from the parametric study are presented and compared with DSM results shown in Table 3.

Table 3: Comparison of FE analysis and DSM ultimate moment estimates

Beam ID	Yield stress (MPa)	λ_l	λ_d	λ_b	M_{nl} (kNm)	M_{nd} (kNm)	M_{ne} (kNm)	M_n (kNm)	M_{FEA} (kNm)	M_{nldg} (kNm)	M_{FEA} / M_n	M_{FEA}/ M_{nldg}
	250	0.82	0.82	0.764	2.411	2.346	2.447	2.346	1.6659	1.5991	0.710	1.042
	350	0.97	0.97	0.904	2.872	2.933	3.161	2.872	1.9852	1.6837	0.691	1.179
LC1	450	1.10	1.1	1.025	3.207	3.441	3.723	3.207	2.1252	1.7502	0.663	1.214
	550	1.22	1.216	1.133	3.44	3.893	4.134	3.44	2.1564	1.8056	0.627	1.194
	590	1.26	1.26	1.173	3.508	4.065	4.256	3.508	2.1553	1.8265	0.614	1.180
	250	0.78	0.788	0.767	2.537	2.462	2.502	2.462	1.801	1.6248	0.731	1.108
	350	0.93	0.932	0.907	3.022	3.088	3.229	3.022	2.024	1.7153	0.670	1.180
LC2	450	1.05	1.057	1.029	3.375	3.63	3.8	3.375	2.278	1.7792	0.675	1.280
	550	1.16	1.168	1.137	3.619	4.113	4.215	3.619	2.435	1.8384	0.673	1.324
	590	1.20	1.21	1.178	3.689	4.294	4.337	3.689	2.653	1.8573	0.719	1.428
	250	0.89	0.898	0.857	2.918	2.923	3.074	2.918	1.7500	1.7426	0.600	1.004
	350	1.06	1.062	1.014	3.406	3.632	3.861	3.406	1.9510	1.8352	0.573	1.063
LC3	450	1.12	1.121	1.15	3.893	4.487	4.397	3.893	1.9864	1.9070	0.510	1.042
	550	1.33	1.332	1.271	3.875	4.794	4.68	3.875	1.9864	1.9679	0.513	1.009
	590	1.37	1.379	1.317	3.898	4.999	4.722	3.898	1.9864	1.9864	0.510	1.000
	250	1.24	1.22	1.226	3.7	4.474	4.363	3.7	1.9302	1.8236	0.522	1.058
	350	1.47	1.446	1.451	3.774	5.471	4.507	3.774	2.3556	1.9187	0.624	1.228
LC4	450	1.66	1.64	1.646	3.774	6.336	4.507	3.774	2.3552	1.9942	0.624	1.181
	550	1.84	1.814	1.819	3.774	7.105	4.507	3.774	2.3685	2.0576	0.628	1.151
	590	1.91	1.877	1.884	3.774	7.397	4.507	3.774	2.3685	2.0806	0.628	1.138
	250	0.90	0.907	0.875	2.372	2.392	2.507	2.372	1.3851	1.3875	0.584	0.998
	350	1.07	1.074	1.034	2.758	2.971	3.131	2.758	1.5979	1.4620	0.579	1.093
LC5	450	1.21	1.217	1.174	2.994	3.471	3.538	2.994	1.6725	1.5180	0.559	1.102
	550	1.34	1.346	1.297	3.101	3.918	3.728	3.101	1.6857	1.5661	0.544	1.076
	590	1.39	1.394	1.344	3.11	4.085	3.744	3.11	1.6862	1.5823	0.542	1.066
	250	0.80	0.803	0.788	2.624	2.564	2.609	2.564	1.6898	1.6388	0.659	1.031
	350	0.94	0.951	0.932	3.114	3.211	3.348	3.114	2.0327	1.7252	0.653	1.178
LC6	450	1.07	1.078	1.057	3.461	3.77	3.914	3.461	2.1999	1.7951	0.636	1.226
	550	1.18	1.192	1.168	3.691	4.27	4.306	3.691	2.2733	1.8516	0.616	1.228
	590	1.23	1.234	1.21	3.753	4.457	4.414	3.753	2.2884	1.8701	0.610	1.224
LC7	250	1.07	1.073	1.073	2.983	3.261	3.356	2.983	1.4247	1.5069	0.478	0.945

	350	1.26	1.27	1.27	3.265	4.012	3.838	3.265	1.5893	1.5867	0.487	1.002
	450	1.43	1.44	1.44	3.297	4.662	3.895	3.297	1.6772	1.6498	0.509	1.017
	550	1.58	1.592	1.592	3.297	5.423	3.895	3.297	1.6565	1.7019	0.502	0.973
	590	1.64	1.649	1.649	3.297	5.46	3.895	3.297	1.6561	1.7213	0.502	0.962
	250	0.81	0.82	0.815	3.545	3.501	3.556	3.501	2.302	2.1369	0.658	1.077
	350	0.96	0.97	0.964	4.183	4.378	4.529	4.183	2.685	2.2534	0.642	1.192
LC8	450	1.09	1.1	1.093	4.619	5.136	5.244	4.619	2.950	2.3436	0.639	1.259
	550	1.21	1.216	1.208	4.887	5.814	5.702	4.887	3.167	2.4192	0.648	1.309
	590	1.24	1.26	1.251	4.951	6.068	5.813	4.951	3.251	2.4468	0.657	1.328
	250	1.00	1.008	0.995	3.084	3.27	3.396	3.084	1.962	1.6419	0.636	1.195
	350	1.19	1.192	1.177	3.465	4.037	4.034	3.465	2.039	1.7282	0.589	1.180
LC9	450	1.35	1.352	1.335	3.593	4.7	4.259	3.593	2.330	1.7969	0.648	1.296
	550	1.49	1.495	1.476	3.594	5.293	4.26	3.594	2.430	1.8521	0.676	1.312
	590	1.54	1.548	1.528	3.594	5.514	4.26	3.594	2.582	1.8750	0.718	1.377
	250	1.19	1.199	1.19	3.502	4.108	4.063	3.502	2.2591	1.7338	0.645	1.303
	350	1.41	1.418	1.408	3.613	5.03	4.256	3.613	2.2816	1.8262	0.632	1.249
LC10	450	1.59	1.608	1.596	3.614	5.828	4.256	3.614	2.2816	1.8996	0.631	1.201
	550	1.76	1.777	1.765	3.614	6.541	4.256	3.614	2.2816	1.9599	0.631	1.164
	590	1.83	1.841	1.828	3.614	6.807	4.256	3.614	2.2816	1.9807	0.631	1.152
	250	0.76	0.76	0.722	2.028	1.995	2.028	1.995	1.3493	1.4249	0.676	0.947
	350	0.89	0.9	0.854	2.507	2.509	2.647	2.507	1.6379	1.5049	0.653	1.088
LC11	450	1.01	1.02	0.968	2.825	2.954	3.156	2.825	1.8164	1.5629	0.643	1.162
	550	1.12	1.128	1.071	3.061	3.351	3.555	3.061	1.9019	1.6145	0.621	1.178
	590	1.16	1.168	1.109	3.135	3.5	3.697	3.135	1.9185	1.6325	0.612	1.175
	250	0.82	0.821	0.801	2.709	2.661	2.725	2.661	1.4117	1.6727	0.531	0.844
	350	0.97	0.971	0.947	3.206	3.327	3.485	3.206	1.6940	1.7681	0.528	0.958
LC12	450	1.10	1.101	1.074	3.552	3.903	4.056	3.552	1.8541	1.8362	0.522	1.010
	550	1.21	1.217	1.187	3.773	4.418	4.438	3.773	1.9294	1.8971	0.511	1.017
	590	1.25	1.261	1.230	3.830	4.609	4.538	3.83	1.9456	1.9142	0.508	1.016
						Mean					0.607	1.1353
						Std. Dev					0.066	0.1246
						Capacity reduction factor (φ)					0.528	0.986

Almostst all the specimens in the parametric study failed in combined local, distortional and lateral-torsional buckling. The response of the beam at failure moment from FE analysis for some of the sections are shown in Fig. 6. From the Table 3, it is notiched that the ultimate moment of the selected beams are strongly influenced by the buckling interaction.

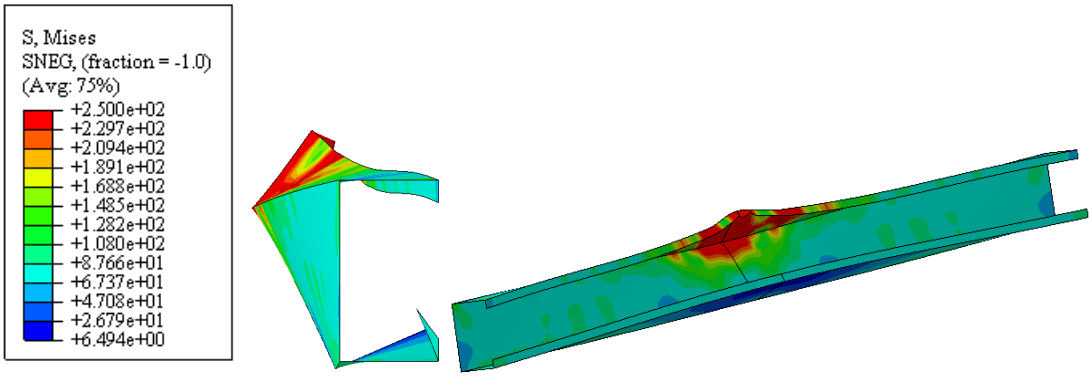

(a) For 120x65x15 - f_y =250 MPa

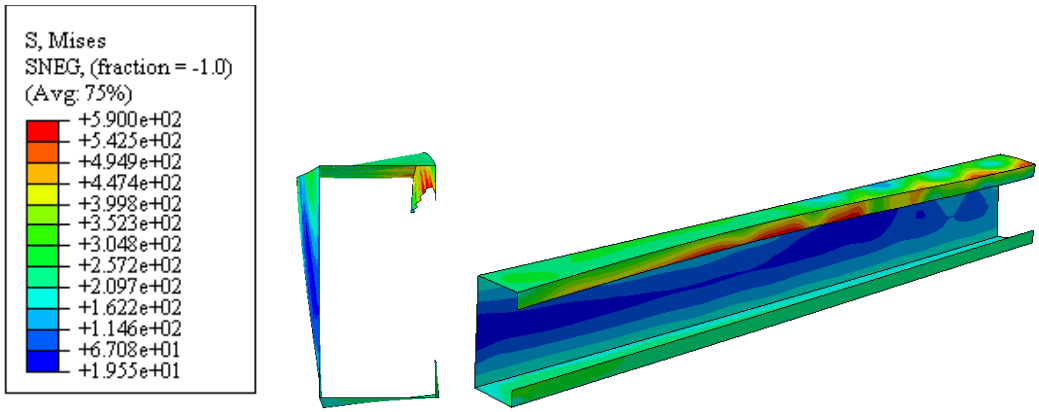

b) For 100x50x15 - f_y =590 MPa

Fig. 6 Von-Misses stress contour at ultimate load

4. DISCUSSION AND DESIGN FORMULATIONS

The nominal flexural strength M_n = Min of (M_{nl}, M_{nd}, M_{ne} and M_{nlde}) for the sections which have their elastic L, D and LT buckling moments nearly equal. The proposed nominal flexural strength (M_{nlde}) for local-distortional-lateral-torsional buckling moment interaction is suggested as shown in Eqn.1. The proposed equation can be considered in addition to the normal equations for the sections which have their elastic L, D and LT buckling moments nearly equal.

$$M_{nlde} = \begin{cases} M_y & \text{for } \lambda_b \leq 0.570 \\ \left(0.3858 * \left(\frac{M_y}{M_{cre}}\right)^{-0.845}\right) M_y & \text{for } \lambda_b > 0.570 \end{cases} \quad (1)$$

where $\lambda_b = \sqrt{M_y/M_{cre}}$ and M_{cre}= Critical elastic global buckling moment.

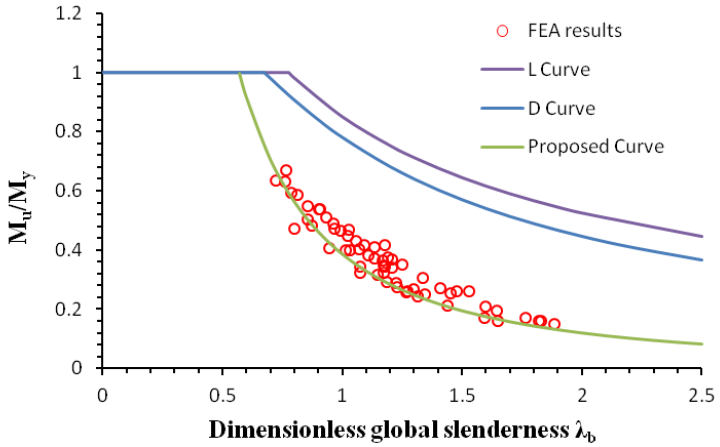

Fig. 7 DSM design curves and variation of M_u/M_y values with the global slenderness

LT buckling plays the key role because it has no post critical strength but the L and D buckling play a secondary role because their post critical strength is not as low as the LT one, therefore the equation was proposed based on critical moments due to LT buckling and also the critical moments due to L, D and LT are nearly equal.

The mean, standard deviation and capacity reduction factor (Φ) values of the ratios of the ultimate moment resistance from FE analysis to the DSM strength prediction and proposed equation were calculated, i.e.,. M_{FEA}/ M_n and M_{FEA}/ M_{nldg} are presented in Table 3. It is shown that the strengths predicted by using the proposed equation are more conservative. Fig. 7 and 8 show the comparison between the ultimate numerical moments and corresponding DSM estimates. The comparisons highlighted the shortcomings in the current DSM results, and the current DSM results are on the unsafe side. But the proposed equations estimates are on the safer side. But several of them are overly conservative. The current and proposed design rules are assessed by using the reliability analysis based on the NAS specifications (AISI-S 100-2007) for cold formed steel structures.

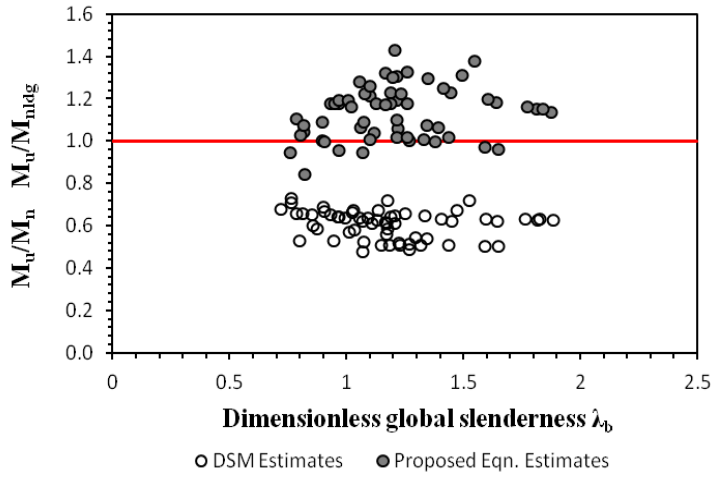

Fig. 8 Variation of M_u/M_n and M_u/M_{nldg} with global slenderness

The reliability analysis followed in this study as reported by Anbarasu (2016). Table 3 compares the FE analysis results with existing and proposed design equations for lipped channel beams. The mean value, standard deviation and the capacity reduction factor, according to existing DSM is 0.607, 0.066 and 0.528, but according to the proposed equation is 1.135, 0.124 and 0.986 respectively. The existing DSM is unreliable, but the modified proposals of DSM equations for the L-D-LT buckling interaction achieve improved accuracy in the design rule.

5. CONCLUSION

This work reported the numerical investigation on the influence of L-D-LT interaction on the buckling behaviour, ultimate strength and design of cold-formed steel lipped channel beams subjected to uniform bending. All the beams analyzed had geometries are selected to ensure the almost equal L-D-LT buckling stress. ABAQUS shell FE analysis was employed to assess the structural response of beams. The following conclusions were extracted from the limitation of the current study:

1. The FE analysis results are generally in reasonable agreement with test results. Therefore, the developed finite element model capably simulated the behaviour of the beams, can be effectively be used to study the behavior of cold-formed lipped channel beams.
2. The current DSM (M_n) flexural strength estimates are unconservative and highly unsafe. It confirms the inadequacy of the current DSM provisions in predicting the flexural strength of beams experiencing L–D–LT interaction and not satisfied the reliability condition and the results showed that the sections failed prematurely. The mean and standard deviation of M_u/M_n are 0.607, 0.066 respectively.
3. Design proposals to the DSM buckling interaction strength curve were presented and discussed. The proposed strength curve was generally conservative, accounting for L-D-LT interaction effects, provides almost always safe ultimate moment estimates but several of them are overly conservative.
4. Also, it is found that the M_{nldg} estimates, reliability factor satisfies the reliability condition. The mean and standard deviation of M_u/M_{nldg} are 1.135, 0.124 respectively.

It is worth to mention that the proposed equation is valid only for lipped channel beams which have their elastic local, distortional and lateral-torsional buckling moments are equal. Furthermore the applicability of the current proposal for L-D–LT interaction equation verification with experimental work is highly encouraged.

NOMENCLATURE

A = cross-sectional area (mm^2)
b = flange width (mm)
d = lip depth (mm)
E = Young's modulus of elasticity (MPa)
f_y = Yield stress (MPa)

h = web depth (mm)
L = Length of column (mm)
M_{crd} = Critical elastic distortional buckling moment (kNm)
M_{cre} = Critical elastic lateral-torsional buckling moment (kNm)
M_{crl} = Critical elastic local buckling moment (kNm)
M_n = Nominal flexural strength (kNm)
M_{nd} = Nominal flexural strength for distortional buckling (kNm)
M_{ne} = Nominal flexural strength for Eulers buckling (kNm)
M_{nl} = Nominal flexural strength for local buckling (kNm)
M_{nlde} = Nominal interaction flexural strength (kNm) accounting for local-distortional-global buckling moment
M_{FEA} = Ultimate moment capacity obtained from finite element analysis (kNm)
$M_{u,test}$ = Ultimate moment capacity obtained from experiment (kNm)
M_y = Yield moment capacity (kNm)
t = thickness (mm)
φ = capacity reduction factor
λ_l = Local slenderness
λ_d = Distortional slenderness
λ_c = Global slenderness

REFERENCES

1. Put BM, Pi YL and Trahair NS. Lateral buckling tests on cold-formed channel beams, *Journal of Structural Engineering, ASCE*, No. 5, **125**(1999) 532-9.
2. Pi YL, Put BM, Trahair NS. Lateral buckling strengths of cold-formed channel section beams, *Journal of Structural Engineering, ASCE*, No. 10, **124**(1998) 1182-91.
3. Yu C, Schafer BW. Local buckling tests on cold-formed steel beams, *Journal of Structural Engineering, ASCE*, No. 12, **129**(2003) 1596-1606.
4. Yu C, Schafer BW. Distortional buckling tests on cold-formed steel beams, *Journal of Structural Engineering, ASCE*, No. 4, **132**(2006) 1-14.
5. Yu C, Schafer BW. Simulation of cold-formed steel beams in local and distortional buckling with applications to direct strength method, *Journal of Constructional Steel Research*, No. 5, **63**(2007) 581-90.
6. Silvestre N, Camotim D. Distortional buckling formulae for cold-formed steel C and Z-section members Part I-Derivation, *Thin-Walled Structures*, **42**(2004) 1567-97.
7. Schafer BW. Review the direct strength method of cold-formed steel member design, *Journal of Constructional Steel Research*, **64**(2008) 766-78.
8. Kurniawan C, Mahendran M. Lateral buckling strength of simply supported lite steel beams subject to moment gradient effects, *Journal of Structural Engineering*, No. 9, **135**(2009) 1058-67.
9. Dinis PB, Camotim D. Local/distortional mode interaction in cold-formed steel lipped channel beams, *Thin-Walled Structures*, **48**(2010) 771-85.
10. Nandini P, Kalyanaraman V. Strength of cold-formed lipped channel beams under

interaction of local, distortional and lateral torsional buckling, *Thin-Walled Structures*, **48**(2010) 872-7.
11. Kankanamge ND, Mahendran M. Behaviour and design of cold-formed steel beams subject to lateral - torsional buckling, *Thin-walled structures*, **51**(2012) 25-38.
12. Laím L, Rodrigues JPC, Silva LS. Flexural behaviour of cold-formed steel beams, *DFE 2013 - International Conference on Design, Fabrication and Economy of Metal Structures*, (2013) pp. 133-138.
13. Niu S, Rasmussen K, Fan F. Distortional - global interaction buckling of stainless steel C-beams: Part I - Experimental investigation, *Journal of Constructional Steel Research*, **96**(2014) 127-39.
14. Kandasamy R, Thenmozhi R, Jayagopal LS. Flexural-torsional-buckling tests of cold-formed lipped channel beams under restrained boundary conditions, *KSCE Journal of Civil Engineering*, No. 7, **19**(2015) 2134-43.
15. Anbarasu M. Local-distortional buckling interaction on cold-formed steel lipped channel beams, *Thin-Walled Structures*, **98**(2016) 351-9.
16. Szymczak CK, Kujawa M. On local buckling of cold-formed channel members, *Thin Walled Structures*, **106**(2016) 93-101.
17. Kankanamge ND. Structural behaviour and design of cold-formed steel beams at elevated temperatures, Ph.D. Thesis, Queensland University of Technology, Brisbane, Australia, 2010.
18. Bebiano R, Silvestre N, Camotim D. GBTUL 2.0β – code for buckling and vibration analysis of thin-walled members, freely available at http://www.civil.ist.utl.pt/gbt, 2008.
19. Schafer BW. CUFSM 3.12, elastic buckling analysis of thin-walled members by finite strip analysis. ⟨/www.ce.jhu.edu/bschafer/cufsm⟩, 2006.
20. AISI-S100: 2007 – North American Specification for the Design of Cold-Formed Steel Structural members Specifications, Washington, DC, U.S.A, 2007.
21. Simulia Inc. Abaqus Standard (Version 6.10), 2008.
22. Schafer BW, Pekoz T. Computational modelling of cold-formed steel: characterizing geometric imperfections and residual stresses, *Journal of Constructional Steel Research*, **47**(1998) 193-210.